

# Modeling and Analysis of 2-Tier Heterogeneous Vehicular Networks Leveraging Roadside Units and Vehicle Relays

Chang-Sik Choi and François Baccelli

## Abstract

While roadside units (RSUs) play an essential role in vehicle-to-everything (V2X) by communicating with users, some users in congestion areas may not be well-served due to data traffic, signal attenuation, and interference. In these cases, vehicle relays can be employed to enhance the network topology to better serve those users. This paper leverages stochastic geometry to propose a novel framework for the performance analysis of heterogeneous vehicular networks with RSUs, vehicle relays, and vehicle users. We present a two-dimensional analytical model where the spatial dependence between RSUs, vehicle relays, vehicle users, and roads is accurately taken into account through a Cox point process structure. Assuming relays are backhauled to RSUs over a reserved wireless resource and users are associated with the closest RSU or relay, we derive the probability that the typical user is associated with either an RSU or a relay. Then, we derive the signal-to-interference ratio (SIR) coverage probability of the typical user. Finally, using the derived formulas, we evaluate the average effective rate of the typical user in the network. This allows us to determine the gain of the average effective rate of users that results from the deployment of relays in the network.

## I. INTRODUCTION

### A. Background and Motivation

Recent innovations have made it possible for vehicular mobility to play new roles in urban environments, extending its traditional transportation role [1]–[3]. Vehicles will participate in

Chang-Sik Choi is with Hongik University, South Korea. François Baccelli is with Inria Paris and Telecom Paris, France. (email: [chang-sik.choi@hongik.ac.kr](mailto:chang-sik.choi@hongik.ac.kr), [francois.baccelli@inria.fr](mailto:francois.baccelli@inria.fr)).

The work of Chang-Sik Choi was supported in part by the NRF-2021R1F1A1059666 and by IITP Grant 2018-0-00792. The work of Francois Baccelli was supported in part by the Simons Foundation grant 197982 and by the ERC NEMO grant 788851 to INRIA.

various road safety and efficiency applications by communicating with neighboring vehicles, pedestrians, traffic lights, Internet-of-Things (IoT) devices, and so on [1], [3]. Advanced vehicles and their sensors provide ways to improve not only the safety of vehicles [4], [5], but also that of others, such as pedestrians [6], [7]. This innovative use of vehicles requires reliable communications among network elements such as vehicles, base stations, smart sensors, and pedestrians [8]–[10].

Vehicular networks featuring reliable and high capacity links can be enabled by deploying base stations close to roads [1]. These nodes are referred to as RSUs in this paper. They will be connected to the core network through a backhaul and will employ advanced V2X communication technologies [11], [12]. Due to their close distances to roads, RSUs are expected to enable various V2X applications [13]–[15]. However, as the number of V2X devices increases and vehicular networks support various services, some users may suffer from limited service because of data congestion, signal attenuation, and high interference [16]. To overcome these limitations, various technologies were proposed. One viable approach is to employ vehicle relays [13]–[19], where vehicle relays are connected to RSUs through a dedicated wireless resource to serve proximal vehicle users or pedestrians. These relays enhance the topology of vehicular networks and benefit to the networks in multiple ways [20]. For instance, users in dense areas can communicate directly with relays, instead of waiting for RSUs. Similarly, when users away from RSUs cannot receive their safety messages, the relays can forward these messages to such users. In positioning applications [12], some vehicles may not receive positioning reference signals (PRSs) from RSUs due to blockages. In this case, vehicle relays can forward the PRSs of RSUs to those vehicles.

This paper aims to analyze the basic performance of such topological enhancement of vehicular networks. First, we use a stochastic geometry model to characterize the spatial distributions of RSUs, vehicle relays, and vehicle users by focusing on the fact that they are all geometrically close to roads [21], [22]. Many analytical studies utilized spatially correlated analytical models including parallel Poisson point processes [23], Poisson processes on Manhattan road systems [24], and Poisson line-based Poisson point processes, i.e., Cox point process [22], [25]. In particular, Poisson Cox models were considered in [26]–[31] to characterize the spatial distribution of vehicles and analyze the basic performance of vehicular users. The Cox point process has points only on lines that are randomly distributed on the plane. By leveraging the conditional structure of the Cox point process, this paper analyzes a heterogeneous vehicular network architecture where 2-tier heterogeneous transmitters exist, namely RSUs and vehicle relays.

TABLE I  
STOCHASTIC GEOMETRY MODEL FOR HETEROGENEOUS NETWORKS

Network	Spatial model
Cellular [32]	Poisson point processes
Vehicular [26]	Poisson and Cox point processes
Vehicular [This paper]	Cox and Cox point processes

While the studies on heterogeneous networks [32] used Poisson point processes assuming independence of network elements, our Cox-based framework incorporates the spatial dependence between heterogeneous network elements such as roads, RSUs, vehicle relays, and vehicle users. Table I depicts the stochastic geometry models for the class of heterogeneous networks considered in the present paper. Using the proposed model, we analyze the user behavior and link reliability, by deriving the association probability of the typical users and by obtaining the SIR distributions of all typical types of communications. We derive the average effective user rate, compare it to the average effective user rate without any relay, and then analyze the gain in effective rates as a function of densities. To the best of the authors' knowledge, the proposed model and the derived results are new.

### B. Theoretical Contributions

**Tractable modeling of heterogeneous vehicular networks with spatial correlation:** in this paper, we characterize the spatial correlation between RSUs, relays, and users by modeling them as Cox point processes generated on the same Poisson line process. The proposed Cox point process is stationary and time-invariant; the proposed framework allows us to investigate not only the statistical average of all users but also the temporal average of a given user. In the proposed network model, both RSUs and relays serve users on the lines. We investigate the association regions for such users. They correspond to the Cox-Voronoi cells of the RSU and relay point process. The proposed network geometry is tractable because RSUs and relays serve users on a wireless spectrum and the relays are served by RSUs over a dedicated wireless spectrum.

**SIR coverage probability and user association probability:** using the stationarity of the user Cox point process, we analyze the typical performance seen by the typical user at the origin. Specifically, under the Palm distribution of the user point process, the typical user is located at the origin and there exists a line containing the origin and hence the RSUs and relays point

processes located on this line; these points create additional interference seen by the typical user. By assuming that the typical user associates with the closest transmitter, we derive the probability that the typical user at the origin is associated with either an RSU or a relay. Based on the association transmitter type, we derive the Laplace transform of the typical interference and then obtain the expression for the SIR distribution of the typical user. We check that the derived formulas match the numerical results simulated by the Monte Carlo experiments.

**Geometric characterization of link types and average effective rate:** leveraging the proposed framework, we derive formulas for the all types of links present in the network. For instance, we obtain the SIR distribution of the users associating with RSUs or relays on different lines. Similarly, we obtain the SIR distribution of the users associating with RSUs or relays on the same line. These formulas give the reliability of each specific type of link as a function of network parameters, including transmit powers, relay or RSU densities, and the path loss exponents.

**Average effective rate of users and potential gain brought by vehicle relays:** We define the average effective link rate based on the mean Shannon rate divided by mean associated number of network elements. We derive the average effective rate of the typical user as a function of the SIR distributions of all typical links and their corresponding bandwidths. We show that, when the RSU-to-relay bandwidth is sufficiently large, vehicle relays will be able to significantly increase the effective rate of users.

## II. SYSTEM MODEL

This section presents the spatial model for the proposed vehicular network with RSUs and vehicle relays. We introduce the propagation model, the association assumption, the relaying protocol, and some performance metrics.

### A. Spatial Model

To represent road geometries observed in some urban area, we assume that the road layout is modeled as an isotropic Poisson line process  $\Phi$  [33]. Specifically, the Poisson line process is generated from a homogeneous Poisson point process on a cylinder set  $\mathbf{C}$  [33]. Consider a Poisson point process  $\chi$  of intensity  $\lambda_l/\pi$  on  $\mathbf{C}$ . Each of its point  $(r, \theta)$  is mapped into a line on the Euclidean plane, where  $r$  corresponds to the distance from the origin to the line and  $\theta$  corresponds to the angle between the line and the  $x$ -axis, measured in the counterclockwise

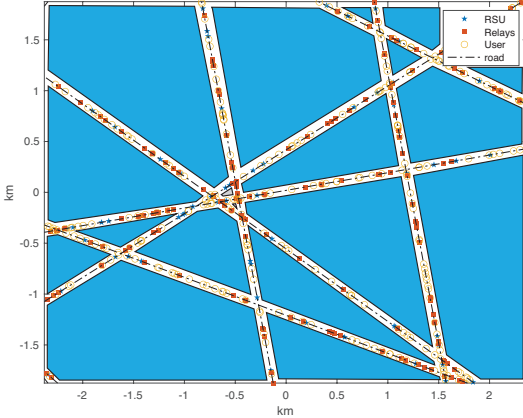


Fig. 1. Illustration of RSUs, relays, and users in the proposed network. The road layout is the Poisson line process. RSUs, relays, and users are the Cox point processes conditional on the same line process. Here,  $\lambda_l = 3/\text{km}$ .  $\mu_s = 2/\text{km}$ ,  $\mu_r = 5/\text{km}$ ,  $\mu_u = 10/\text{km}$ . Colored polygons represent building surfaces and walls in urban areas.

direction. Since  $\chi$  is a homogeneous Poisson, we have an isotropic Poisson line process  $\Phi$  on the Euclidean plane. The choice of intensity measure  $\chi$  determines the way that lines are created on the plane. For instance, concentrating the angular component on 0 and  $\pi/2$  gives a Manhattan-like road structure, where lines are parallel to the  $x$  and  $y$ -axes. The analysis of other scenarios such as this Poisson Manhattan case is possible but is left for future research.

The value of  $\lambda_l$  determines the average number of lines that intersect a disk of diameter 1 [33]. As a result, by changing the value of  $\lambda_l$ , one can easily introduce more or less lines on the Euclidean plane. Fig. 1 depicts the Poisson line process as dashed lines. It shows that network elements such as RSUs, relays, and users are all located on these lines.

Conditionally on each line  $l(r, \theta) \in \Phi$ , the locations of RSUs, vehicle relays, and vehicle users, are modeled as independent one-dimensional Poisson point processes  $S_{r, \theta}$ ,  $R_{r, \theta}$ , and  $U_{r, \theta}$  of intensities  $\mu_s$ ,  $\mu_r$ , and  $\mu_u$ , respectively. (see Fig. 1 where RSUs, vehicle relays, and vehicle users are depicted by stars, squares, and circles, respectively). Collectively, the RSU point process, the relay point process, and the user point process—denoted by  $S$ ,  $R$ , and  $U$ —form Cox point processes based on a single Poisson line process. Table II summarizes the proposed model and the notation.

We assume  $\mu_u \gg \mu_s$ , meaning the network is dense. In this case, RSUs always have users to serve with high probability. Similarly, we assume that the densities of RSUs and relays are

TABLE II  
NETWORK ELEMENTS

Variable	Description	Model
$\Phi$	Road structure	2-D Poisson line
$S_{r,\theta}$	RSUs on line $l(r, \theta)$	1-D Poisson ( $\mu_s$ )
$R_{r,\theta}$	Relays on line $l(r, \theta)$	1-D Poisson ( $\mu_r$ )
$U_{r,\theta}$	User on line $l(r, \theta)$	1-D Poisson ( $\mu_u$ )
$S = \bigcup_{r_i, \theta_i \in \Phi} S_{r_i, \theta_i}$	RSUs on lines	2-D Cox ( $\lambda_l \mu_s$ )
$R = \bigcup_{r_i, \theta_i \in \Phi} R_{r_i, \theta_i}$	Relays on lines	2-D Cox ( $\lambda_l \mu_r$ )
$U = \bigcup_{r, \theta \in \Phi} U_{r, \theta}$	Users on lines	2-D Cox ( $\lambda_l \mu_u$ )

comparable and that relays have users to serve with high probability. We assume that vehicle relays and vehicle users move at constant speeds  $v_r$ , and  $v_u$  along the lines on which they are located. This ensures the preservation of the conditional Poisson property of the relay and user point processes [34]. Note that the analysis of this paper holds for any other dynamics as long as the locations of relays and users on each line are Poisson point processes at any given time. One such example is that where vehicles choosing their own speeds using an independent and identical distribution.

### B. Propagation Model

Consider a receiver located at a distance  $d$  from its transmitter. In the proposed heterogeneous vehicular network, transmitters are either RSUs or vehicle relays. To capture rich scattering around the users and path loss characteristics based on geometry of links [35]–[37], the received signal power at the receiver is assumed to be of the form  $pHL(d)$  where  $p = \{p_s, p_r\}$  is the transmit power of an RSU and a relay, respectively,  $H$  represents Rayleigh fading, modeled by an independent exponential random variable with average one, and  $L(d)$  is the path loss over distance  $d$ . We assume that the transmit powers for RSUs and relays are given by  $p_s$  and  $p_r$ , respectively. Specifically, as in [37]–[39], the path loss has different behaviors depending on the relative geometry of transmitter and receiver, or more precisely on whether they are on the same road or not. More precisely, we assume that a power-law based path loss over a distance  $d$  is given by

$$L(d) = \begin{cases} d^{-\alpha} & \text{on the same line,} \\ d^{-\beta} & \text{on different lines,} \end{cases} \quad (1)$$

where  $2 < \alpha \leq \beta$ . Thanks to the above assumption, we identify and analyze cross-road and inter-road communications in heterogeneous vehicular networks.

### C. User Association and Relay Association

In the proposed networks, transmitters are RSUs and relays. We assume that each user is associated with its closest transmitter, namely either an RSU or a relay. The proposed nearest association considers the fact that, in safety-related V2X applications [1], RSUs or vehicle transmitters broadcast their basic safety messages to geometrically close receivers. The analysis of the maximum average power association is left for future work. Fig. 3 depicts the user association. In each cell, users are connected to the transmitter at the center of the cell. The nearest association produces the association areas that correspond to the Voronoi tessellation w.r.t.  $S + R$ —the RSU and relay Cox point processes [25], [40].

We assume that in order to serve users, relays are connected to the RSUs through a wireless backhaul. We assume relays are associated with their nearest RSUs.

Figure 2 shows the hierarchical structure of the proposed heterogeneous vehicular network where RSUs and relays serve users.

### D. Dedicated Resource for Relays

The communications involving users, namely RSU-to-user links and relay-to-user links, are assumed to occupy a wireless spectrum of bandwidth  $W_1$ . We assume that RSU-to-relay links use a disjoint wireless spectrum of width  $W_2$ . Hence, RSU-to-relay communications do not interfere with the user-related communications such as RSU-to-user and relay-to-user ones [41].

### E. Performance Metrics

This paper analyzes the performance seen by users. First, we analyze the SIR distribution of the typical user located at the origin. Combining this with the user association probability, we characterize the different types of communications present in the network. We also analyze the SIR distribution of the typical relay. We use this to quantify the impact of the RSU-to-relay communications in terms of the user effective rate.

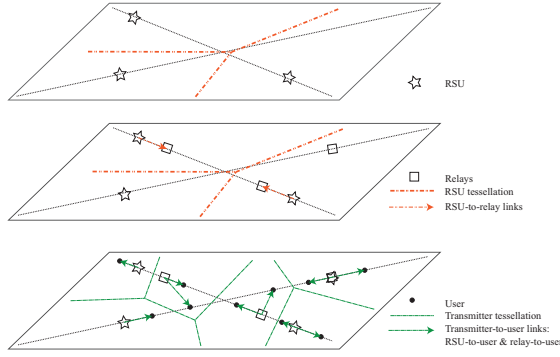


Fig. 2. Illustration of the proposed vehicular architecture. In this figure only, we present RSUs (pentagrams), relays (squares), and users (circles) on three separate planes to describe the proposed hierarchical structure. RSUs transmit to users. Relays receive from RSU and transmit to users close to them. Users are associated with their closest transmitters, namely either RSUs or relays. Double dashed arrows are RSU-to-relay links and single dashed arrows are RSU-to-user and relay-to-user links. Note that RSU-to-relay links use a dedicated spectrum of bandwidth  $W_2$ . The RSU tessellation indicates the relay association boundary. On the other hand, the transmitter tessellation indicates the user association boundary.

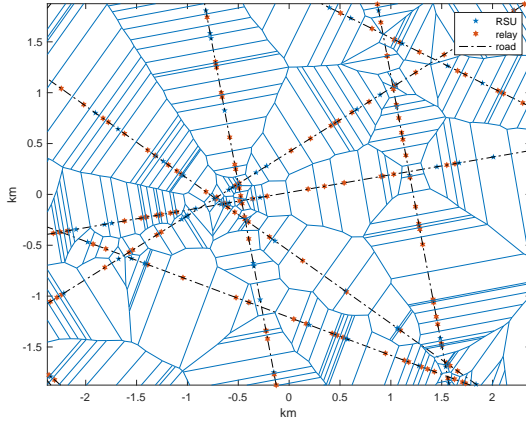


Fig. 3. Illustration of the user association region. Here  $\lambda_l = 3/\text{km}$ ,  $\mu_s = 2/\text{km}$ , and  $\mu_r = 5/\text{km}$ . The user association regions correspond to the Voronoi tessellation with respect to the transmitter point process: RSU plus relay Cox point processes. In each Voronoi cell, users are associated with the transmitter at the center of the cell.

1) *SIR distribution of typical user*: To analyze the SIR distribution of the typical user, we use the Palm distribution of the user point process,  $\mathbf{P}_U^0(\cdot)$ . This features a typical user at the origin. Therefore a line  $l(0, \theta_0)$  almost surely exists with a RSU point process  $S_{0, \theta_0}$ , and a relay point process  $R_{0, \theta_0}$  on it [22], [25]. Consequently, the interference from this line should be considered.

The SIR distribution of the typical user  $\mathbf{P}_U^0(\text{SIR} > \tau)$  is

$$\mathbf{P}_U^0 \left( \frac{pHL(\|X^*\|)}{\sum_{X_j \in S+R \setminus B(\|X^*\|)} p_{X_j} H_j L(\|X_j\|)} > \tau \right), \quad (2)$$

where  $p$  is the transmit power of the association transmitter which could be either  $p_s$  or  $p_r$  depending on the association. We denote by  $B_0(\|X^*\|)$  the ball of radius  $\|X^*\|$  centered at the origin. We also write  $B_0(r) = B(r)$ . Here,  $\tau$  is the SIR threshold. Based on the association principle of Section II-C, the association transmitter  $X^*$  is given by

$$X^* = \arg \min_{X_k \in S_{0,\theta} + R_{0,\theta} + S + R} \|X_k\|. \quad (3)$$

Here, the association transmitter is selected out of the point processes:  $S_{0,\theta_0}$ ,  $R_{0,\theta_0}$ ,  $S$ , and  $R$ . When the association transmitter is a RSU, we write  $X^* = X_S^*$ . When the association transmitter is a relay, we write  $X^* = X_R^*$ .

Based on the proposed association principle, users can be divided into two categories, namely those associated with RSUs and those associated with relays. Since there are various types of links in the proposed network, a separate evaluation of each type will be provided.

The SIR distributions of each type are

$$\mathbf{P}_U^0(\text{SIR}_{S \rightarrow U} > \tau) := \mathbf{P}_U^0(\text{SIR} > \tau | X^* = X_S^*), \quad (4)$$

$$\mathbf{P}_U^0(\text{SIR}_{R \rightarrow U} > \tau) := \mathbf{P}_U^0(\text{SIR} > \tau | X^* = X_R^*), \quad (5)$$

where the former denotes the SIR distribution of the typical relay-associated user and the latter denotes that of the typical RSU-associated user.

2) *SIR of typical relays and effective rate of the typical user:* To analyze the SIR of the typical relay, we consider the Palm distribution of the relay point process. The SIR distribution of the typical relay,  $\mathbf{P}_R^0(\text{SIR}_{S \rightarrow R} > \tau)$  is given by

$$\mathbf{P}_R^0 \left( \frac{p_s HL(\|X_S^*\|)}{\sum_{X_j \in S \setminus B(\|X_S^*\|)} p_s H_j L(\|X_j\|)} > \tau \right), \quad (6)$$

where  $X_S^*$  is the RSU closest to the typical relay located at the origin under the Palm distribution of the relay point process  $R$ . Since RSU-to-relay communications are assumed to occur on a dedicated resource of bandwidth  $W_2$ , the typical relay receives no interference from the RSU-to-user and relay-to-user communications. Leveraging the SIR distribution of the typical relay in Eq. (6), we can quantify the impact of RSU-to-relay links onto the relay-associated users,

by deriving the average effective rates of different links. The precise definition of the average effective rate will be given in Section III-D.

The RSU-to-relays links do not directly determine the network performance seen from users. However, these links indirectly affect the user performance by restricting the amount of data rate available at relays. Consequently, the throughput of relay-associated users will be determined by (i) the throughput of RSU-to-relay links and (ii) the throughput of relay-to-user links, and (iii) the bandwidths  $W_1$  and  $W_2$ . We will see this closely in Section III-D.

### III. MAIN RESULTS

Section III-A gives the association probability of the typical user. Section III-B analyzes the SIR distribution of the typical user. Section III-C computes the SIR distribution of the typical relay. Section III-D evaluates the average effective rate of the typical user.

#### A. Association of the Typical User

As described in Section II, each user has either a RSU association or a relay association, depending on its distances to RSUs and relays. Here, we study the probability that the typical user is associated with either an RSU or a relay. The association probability is derived under the Palm distribution of the user point process. This determines the fraction of users associated with RSUs and with relays.

**Theorem 1.** *The probability that the typical user is associated with an RSU is given by*

$$\begin{aligned} \mathbf{P}(A_s) = & \int_0^\infty 2\mu_s \exp \left( -2(\mu_s + \mu_r)r - 2\lambda_l \int_0^r 1 - e^{-2(\mu_s + \mu_r)\sqrt{r^2 - u^2}} du \right) dr \\ & + 4\mu_s \lambda_l \int_0^\infty \int_0^{\pi/2} r e^{-2r(\mu_s + \mu_r) - 2r(\mu_s + \mu_r) \sin(\theta) - 2\lambda_l \int_0^r 1 - \exp(-2(\mu_s + \mu_r)\sqrt{r^2 - u^2}) du} d\theta dr. \end{aligned}$$

*Likewise, the probability that the typical user is associated with a relay is  $\mathbf{P}(A_r) = 1 - \mathbf{P}(A_s)$ .*

*Proof:* We analyze the association probability by considering the typical user at the origin. By the law of total probability, the probability that the typical user is associated with an RSU is

$$\mathbf{P}_U^0(A_s) = \mathbf{P}_U^0(A_s, E) + \mathbf{P}_U^0(A_s, E^c), \quad (7)$$

where  $E$  denotes the event that the association RSU and the typical user at the origin are on the same line. Similarly,  $E^c$  denotes the event that the association RSU and typical user is not

on the same line. Conditional on the Poisson line process  $\Phi$  and then on the distance to the association RSU  $\|X_S^*\| = r$ , we have

$$\begin{aligned}\mathbf{P}_U^0(A_s, E) &= \mathbf{E} [\mathbf{P}_U^0(A_s, E|\Phi)] \\ &= \mathbf{E} \left[ \int_{r=0}^{r=\infty} \mathbf{P}_U^0(A_s, E, \|X_S^*\| \in [r, r+dr)|\Phi) \right],\end{aligned}\quad (8)$$

where we have

$$\begin{aligned}\mathbf{P}_U^0(A_s, E, \|X_S^*\| \in (r, r+dr)|\Phi) \\ = \mathbf{P}_U^0(\|X_{S_{0,\theta_0}}^*\| \in (r, r+dr), \|X_{R_{0,\theta_0}}^*\| > r, S + R \setminus (S_{0,\theta_0} + R_{0,\theta_0})(B_0(r)) = 0|\Phi),\end{aligned}\quad (9)$$

where  $X_{S_{0,\theta_0}}^*$  denotes the point of  $S_{0,\theta_0}$  closest to the origin,  $X_{R_{0,\theta_0}}^*$  denotes the point of  $R_{0,\theta_0}$  closest to the origin, and  $S + R \setminus (S_{0,\theta_0} + R_{0,\theta_0})$  denotes the point process  $S + R$  except  $S_{0,\theta_0}$  and  $R_{0,\theta_0}$ . Conditional on  $\Phi$ , the above three terms of Eq. (9) are independent. As a result,

$$\mathbf{P}_U^0(A_s, E, \|X_S^*\| \in [r, r+dr)|\Phi) = 2\mu_s e^{-2\mu_s r} dr e^{-2\mu_r r} \prod_{r_i, \theta_i \in \Phi}^{r_i < r} e^{-2(\mu_s + \mu_r)\sqrt{r^2 - r_i^2}}. \quad (10)$$

Then, by using the probability generating functional of the Poisson line process [33], [42],

$$\mathbf{P}_U^0(A_s, E) = \int_0^\infty 2\mu_s \exp \left( -2(\mu_s + \mu_r)r - 2\lambda_l \int_0^r 1 - e^{-2(\mu_s + \mu_r)\sqrt{r^2 - u^2}} du \right) dr. \quad (11)$$

Similarly, to obtain the second part of Eq. (7), we have

$$\begin{aligned}\mathbf{P}_U^0(A_s, E^c) &= \mathbf{E}_\Phi [\mathbf{P}_U^0(A_s, E^c|\Phi)] \\ &= \mathbf{E}_\Phi [\mathbf{E}_{l_\star} [\mathbf{P}_U^0(A_s, E^c|l_\star, \Phi)]] \\ &= \mathbf{E}_\Phi \left[ \mathbf{E}_{l_\star} \left[ \int \mathbf{P}_U^0(A_s|E^c, \|X_S^*\| = r, l_\star, \Phi) g(r) dr \right] \right],\end{aligned}\quad (12)$$

where  $l_\star$  is the line of the association RSU,  $\|X_S^*\| = r$  is the distance from the origin to the association RSU, and  $g(r)$  is the probability density function of  $E^c$  and  $\|X_S^*\|$ , conditional on  $l_\star$  and  $\Phi$ . We have

$$\begin{aligned}\mathbf{P}_U^0(A_s|E^c, r, l_\star, \Phi) &= \mathbf{P}(R_{r_\star, \theta_\star}(B(r)) = \emptyset) \prod_{l(r_i, \theta_i) \in \Phi + l(r_0, \theta_0)} \mathbf{P}(S_{r_i, \theta_i} + R_{r_i, \theta_i}(B(r)) = \emptyset) \\ &= e^{-2\mu_r \sqrt{r^2 - r_\star^2}} e^{-2(\mu_s + \mu_r)r} \prod_{l(r_i, \theta_i) \in \Phi}^{r_i < r} e^{-2(\mu_s + \mu_r)\sqrt{r^2 - r_i^2}},\end{aligned}\quad (13)$$

where we use the void probability of the Poisson point process.

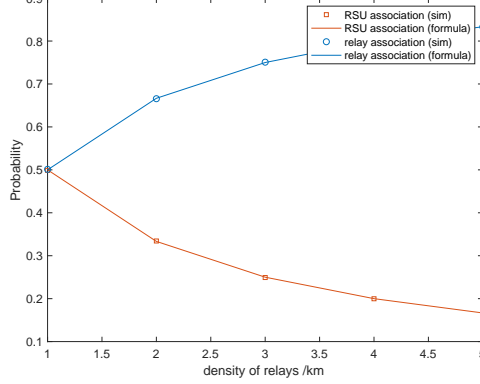


Fig. 4. Illustration of the association probability of the typical user. The derived formula of Theorem 1 matches the simulation results. We use  $\lambda_l = 2/\text{km}$  and  $\mu_s = 1/\text{km}$ .

We have

$$\begin{aligned}
g(r) &= \frac{d}{dr} (\mathbf{P}(\|X_S^*\| \leq r, E^c | l_*, \Phi)) \\
&= \frac{d}{dr} \left( 1 - \mathbf{P} \left( \prod_{X_i \in S_{r_*, \theta_*}} \|X_i\| > r, E^c | l_*, \Phi \right) \right) \\
&= \frac{d}{dr} \left( 1 - e^{-2\mu_s \sqrt{r^2 - r_*^2}} \right) \\
&= \frac{2\mu_s r e^{-2\mu_s \sqrt{r^2 - r_*^2}}}{\sqrt{r^2 - r_*^2}}. \tag{14}
\end{aligned}$$

We use Eqs. (13) (14) in Eq. (12) and use Fubini's theorem to change the order of integrations: we integrate the expression w.r.t.  $l_*$ ,  $\Phi$ , and then  $r$ . First, integrating w.r.t.  $l_*$ , we have

$$\begin{aligned}
\mathbf{E}_{l_*} \left[ \frac{2\mu_s r e^{-2(\mu_s + \mu_r) \sqrt{r^2 - r_*^2}}}{\sqrt{r^2 - r_*^2}} \right] &= 4\mu_s \lambda_l r \int_0^r \frac{e^{-2(\mu_s + \mu_r) \sqrt{r^2 - z^2}}}{\sqrt{r^2 - z^2}} dz \\
&= 4\mu_s \lambda_l r \int_0^{\pi/2} e^{-2r(\mu_s + \mu_r) \sin(\theta)} d\theta, \tag{15}
\end{aligned}$$

where we use Campbell's formula [34]. Then, we integrate the rest of Eqs. (12) and (13) w.r.t.  $\Phi_l$  and then  $r$  to get

$$\mathbf{P}_U^0(A_s, E^c) = 4\mu_s \lambda_l \int_0^\infty \int_0^{\pi/2} r e^{-2r(\mu_s + \mu_r) - 2r(\mu_s + \mu_r) \sin(\theta) - 2\lambda_l \int_0^r 1 - \exp(-2(\mu_s + \mu_r) \sqrt{r^2 - u^2}) du} d\theta dr,$$

We complete the proof by  $\mathbf{P}_U^0(A_s) = \mathbf{P}_U^0(A_s, E) + \mathbf{P}_U^0(A_s, E^c)$ .  $\blacksquare$

Fig. 4 shows that the derived association probability derived in Theorem 1 matches the association probability numerically obtained by the Monte-Carlo simulations. We use  $\lambda_l = 2/\text{km}$ .

We see that as the density of relays increases, the relay association probability increases. Since the user association is based on distance, it is possible that users are associated with RSUs or relays on different lines. We will use the derived association probability to evaluate the SIR distribution of the typical user. In addition, we show that the association probability is not given by a simple ratio of densities, as we have seen in the association of the heterogeneous networks leveraging the Poisson point processes [32]. This occurs because of the spatial correlation between RSUs and relays.

**Proposition 1.** *The mean number of users associated to the typical RSU is  $\frac{\mu_u}{\mu_s} \mathbf{P}_u(A_s)$  and the mean number of users associated to the typical relay is  $\frac{\mu_u}{\mu_r} \mathbf{P}_u^0(A_r)$ . The mean number of relays associated to the typical RSU is  $\frac{\mu_r}{\mu_s}$ .*

*Proof:* Consider a factor graph with an edge from each user to its association RSU or relay. From the mass transport principle [34],

$$\lambda_l \mu_u \mathbf{P}_U^0(A_s, E) = \lambda_l \mu_s d_{\text{in}}, \quad (16)$$

where the LHS is the mean mass sent by the users to their association RSUs on the same lines, whereas the RHS is the mean mass received by the RSUs from their associated users on the same lines.  $\lambda_l \mu_s$  is the spatial density of RSUs and  $d_{\text{in}}$  is the mean number of same-line users associated to the typical RSU under the Palm distribution of  $S$ . Similarly, considering users and their associated RSUs on different lines, we have

$$\lambda_l \mu_u \mathbf{P}_U^0(A_s, E^c) = \lambda_l \mu_s d'_{\text{in}}, \quad (17)$$

where the LHS is the mean mass out of the users and the RHS is the mean mass received by the RSUs:  $d'_{\text{in}}$  is the mean number of different-line users associated to the typical RSU. As a result, the mean number of users per RSU is  $d'_{\text{in}} + d_{\text{in}} = \frac{\mu_u}{\mu_s} \mathbf{P}_U^0(A_s)$ . Similarly, the mean number of users per relay is  $\frac{\mu_u}{\mu_r} \mathbf{P}_U^0(A_r)$ . Finally, the mean number of relays per RSU is  $\frac{\mu_r}{\mu_s}$ .  $\blacksquare$

### B. SIR Distribution of the Typical User

This section gives the SIR distribution of the typical user. Note all RSUs and relays are assumed to have users to serve with high probability. We denote by  $\gamma$  the ratio of relay transmit power to the RSU transmit power,  $\gamma = p_r/p_s$ . As in Section III-B, let  $E$  be the event that the association transmitter and the typical user are on the same line. We denote by  $A_s$  the event that

the association transmitter is an RSU and by  $A_r$  the event that the association transmitter is a relay.

**Theorem 2.** *The SIR distribution of the typical user is given by*

$$\begin{aligned} \mathbf{P}_U^0(SIR > \tau) = & \mathbf{P}_U^0(SIR > \tau, E, A_s) + \mathbf{P}_U^0(SIR > \tau, E, A_r) \\ & + \mathbf{P}_U^0(SIR > \tau, E^c, A_s) + \mathbf{P}_U^0(SIR > \tau, E^c, A_r), \end{aligned} \quad (18)$$

where the first term is the coverage probability with the association RSU being on the line  $l(0, \theta_0)$ , and the second term is the coverage probability with the association relay being on the line  $l(0, \theta_0)$ . Similarly, the third term is the coverage probability with the association RSU not being on  $l(0, \theta_0)$  and the last term is the coverage probability with the association relay not being on  $l(0, \theta_0)$ . We have

$$\begin{aligned} \mathbf{P}_U^0(SIR > \tau, E, A_s) &= \int_0^\infty G_1(r, a, b) e^{-2\lambda_l \int_0^r 1 - G_2(r, v, a, b) dv - 2\lambda_l \int_r^\infty 1 - G_3(r, v, a, b) dv} dr \Big|_{a=1, b=\frac{1}{\gamma}}, \\ \mathbf{P}_U^0(SIR > \tau, E, A_r) &= \int_0^\infty G_1(r, a, b) e^{-2\lambda_l \int_0^r 1 - G_2(r, v, a, b) dv - 2\lambda_l \int_r^\infty 1 - G_3(r, v, a, b) dv} dr \Big|_{a=\gamma, b=1}, \end{aligned}$$

where

$$\begin{aligned} G_1(r, a, b) &= 2\mu_s e^{-2r\mu_s - 2\mu_s \int_r^\infty \frac{\tau r^\alpha u^{-\alpha}}{a + \tau r^\alpha u^{-\alpha}} du - 2\mu_r \int_r^\infty \frac{\tau r^\alpha u^{-\alpha}}{b + \tau r^\alpha u^{-\alpha}} du}, \\ G_2(r, v, a, b) &= e^{-2(\mu_s + \mu_r) \sqrt{r^2 - v^2} - 2\mu_s \int_{\sqrt{r^2 - v^2}}^\infty \frac{\tau r^\alpha (v^2 + u^2)^{-\frac{\beta}{2}}}{a + \tau r^\alpha (v^2 + u^2)^{-\frac{\beta}{2}}} du - 2\mu_r \int_{\sqrt{r^2 - v^2}}^\infty \frac{\tau r^\alpha (v^2 + u^2)^{-\frac{\beta}{2}}}{b + \tau r^\alpha (v^2 + u^2)^{-\frac{\beta}{2}}} du}, \\ G_3(r, v, a, b) &= e^{-2\mu_s \int_0^\infty \frac{\tau r^\alpha (v^2 + u^2)^{-\beta/2}}{a + \tau r^\alpha (v^2 + u^2)^{-\beta/2}} du - 2\mu_r \int_0^\infty \frac{\tau r^\alpha (v^2 + u^2)^{-\beta/2}}{b + \tau r^\alpha (v^2 + u^2)^{-\beta/2}} du}. \end{aligned}$$

On the other hand, the last two terms of Eq. (18), are

$$\begin{aligned} \mathbf{P}_U^0(SIR > \tau, E^c, A_s) &= \int_0^\infty H_1(r, a, b) e^{-2\lambda_l \int_0^r 1 - H_2(r, v, a, b) dv - 2\lambda_l \int_r^\infty 1 - H_3(r, v, a, b) dv} H_4(r, c) dr \Big|_{a=1, b=\frac{1}{\gamma}, c=\mu_s}, \\ \mathbf{P}_U^0(SIR > \tau, E^c, A_r) &= \int_0^\infty H_1(r, a, b) e^{-2\lambda_l \int_0^r 1 - H_2(r, v, a, b) dv - 2\lambda_l \int_r^\infty 1 - H_3(r, v, a, b) dv} H_4(r, c) dr \Big|_{a=\gamma, b=1, c=\mu_r}, \end{aligned}$$

respectively, where

$$\begin{aligned}
H_1(r, a, b) &= e^{-2\mu_s r - 2\mu_s \int_r^\infty \frac{\tau r^\beta u^{-\alpha}}{a + \tau r^\beta u^{-\alpha}} du} - 2\mu_r \int_r^\infty \frac{\tau r^\beta u^{-\alpha}}{b + \tau r^\beta u^{-\alpha}} du, \\
H_2(r, v, a, b) &= e^{-2(\mu_s + \mu_r)\sqrt{r^2 - v^2} - 2\mu_s \int_{\sqrt{r^2 - v^2}}^\infty \frac{\tau r^\beta (v^2 + u^2)^{-\beta/2}}{a + \tau r^\beta (v^2 + u^2)^{-\beta/2}} du} - 2\mu_r \int_{\sqrt{r^2 - v^2}}^\infty \frac{\tau r^\beta (v^2 + u^2)^{-\beta/2}}{b + \tau r^\beta (v^2 + u^2)^{-\beta/2}} du, \\
H_3(r, v, a, b) &= e^{-2\mu_s \int_0^\infty \frac{\tau r^\beta (v^2 + u^2)^{-\beta/2}}{a + \tau r^\beta (v^2 + u^2)^{-\beta/2}} du} - 2\mu_r \int_0^\infty \frac{\tau r^\beta (v^2 + u^2)^{-\beta/2}}{b + \tau r^\beta (v^2 + u^2)^{-\beta/2}} du, \\
H_4(r, c) &= 4\lambda_l c r \int_0^{\pi/2} e^{-2r(\mu_s + \mu_r) \sin(\theta) - 2c \int_{r \sin(\theta)}^\infty \frac{\tau r^\beta (r^2 \cos^2(\theta) + v^2)^{-\beta/2}}{1 + \tau r^\beta (r^2 \cos^2(\theta) + v^2)^{-\beta/2}} dv} d\theta.
\end{aligned}$$

*Proof:* Under the Palm distribution of the user point process,  $\mathbf{P}_U^0(\cdot)$ , there exist a typical user at the origin and a line  $l(0, \theta_0)$  containing the typical user. Here,  $\theta_0$  is a uniform random variable between 0 and  $\pi$ . By the law of total probability, the SIR distribution is given by

$$\mathbf{P}_U^0(\text{SIR} > \tau) = \mathbf{P}_U^0(\text{SIR} > \tau, E) + \mathbf{P}_U^0(\text{SIR} > \tau, E^c), \quad (19)$$

where we can write  $E : \{l_\star = l(0, \theta_0)\}$  and  $E^c : \{l_\star \neq l(0, \theta_0)\}$ . The former is the event that the line  $l_\star$  containing the association transmitter is  $l(0, \theta_0)$ , the line that contains the typical user.

$$\mathbf{P}_U^0(\text{SIR} > \tau, E) = \mathbf{P}_U^0(\text{SIR} > \tau, E, A_s) + \mathbf{P}_U^0(\text{SIR} > \tau, E, A_r), \quad (20)$$

where  $A_s$  and  $A_r$  are the events that the typical user is associated with its closest RSU and with its closest relay, respectively. Then, with  $I$  the interference seen by the typical user, we have

$$\begin{aligned}
&\mathbf{P}(\text{SIR} > \tau, E, A_s) \\
&= \mathbf{P}_U^0(p_s H L(\|X^*\|) > \tau I, E, A_s) \\
&= \mathbf{P}_U^0(p_s H > \tau I \|X_\star\|^\alpha, E, A_s) \\
&= \mathbf{E}_\Phi \left[ \mathbf{P}_U^0 \left( H > \frac{\tau I \|X_\star\|^\alpha}{p_s}, E, A_s \middle| \Phi \right) \right] \\
&= \mathbf{E}_\Phi \left[ \int_{r=0}^{r=\infty} \mathbf{P}_U^0 \left( H > \frac{\tau r^\alpha I}{p_s} \middle| E, A_s, \|X_S^*\| = r, \Phi \right) \mathbf{P}(\|X_S^*\| \in [r, r + dr], E, A_s | \Phi) \right], \quad (21)
\end{aligned}$$

where we express the probability as the conditional expectation w.r.t.  $\Phi$ . Then, we write it as a conditional expectation w.r.t. the nearest RSU. We have  $\mathbf{P}(\|X_S^*\| = r dr, E, A_s | \Phi)$  the conditional probability density function of the distance from the origin to the closest RSU.

In a similar way, we have

$$\begin{aligned} & \mathbf{P}(\text{SIR} > \tau, E, A_r) \\ &= \mathbf{E}_\Phi \left[ \int_{r=0}^{r=\infty} \mathbf{P}_U^0 \left( H > \frac{\tau r^\alpha I}{p_r} \middle| E, A_r, \|X_R^*\| = r, \Phi \right) \mathbf{P}(\|X_R^*\| \in [r, r + dr], E, A_r | \Phi) \right]. \quad (22) \end{aligned}$$

In Eq. (22),  $\mathbf{P}(\|X_R^*\| \in [r, r + dr], E, A_r | \Phi)$  is the conditional probability density function of the distance from the origin to the nearest relay. Furthermore, the integrands of Eqs. (21) and (22) are

$$\mathbf{P}_U^0 \left( H > \frac{\tau r^\alpha I}{p_s} \middle| E, A_s, r, \Phi \right) = \mathbf{E}_U^0 [e^{-sI} | E, A_s, r, \Phi] |_{s=\tau r^\alpha p_s^{-1}}, \quad (23)$$

$$\mathbf{P}_U^0 \left( H > \frac{\tau r^\alpha I}{p_r} \middle| E, A_r, r, \Phi \right) = \mathbf{E}_U^0 [e^{-sI} | E, A_r, r, \Phi] |_{s=\tau r^\alpha p_r^{-1}}, \quad (24)$$

respectively. We obtain  $\mathbf{E}_U^0 [e^{-sI} | E, A_s, r, \Phi] = \mathbf{E}_U^0 [e^{-sI} | E, A_r, r, \Phi]$  from the independence of the Poisson point processes. The conditional Laplace transform of interference is given by

$$\begin{aligned} & \mathbf{E}_U^0 [e^{-sI} | E, A_s, r, \Phi] \\ & \stackrel{(a)}{=} \prod_{T_k \in S_{0,\theta_0} + R_{0,\theta_0}}^{|T_k|>r} \left( \frac{1}{1 + sp\|T_k\|^{-\frac{\beta}{2}}} \right) \prod_{r_i, \theta_i \in \Phi \setminus 0, \theta_0} \left( \prod_{T_k \in S_{r_i,\theta_i} + R_{r_i,\theta_i}}^{|T_k|>r} \frac{1}{1 + sp\|T_k\|^{-\frac{\beta}{2}}} \right) \\ & \stackrel{(b)}{=} \exp \left( -2\mu_s \int_r^\infty \frac{sp_s u^{-\alpha}}{1 + sp_s u^{-\alpha}} du - 2\mu_r \int_r^\infty \frac{sp_r u^{-\alpha}}{1 + sp_r u^{-\alpha}} du \right) \\ & \quad \times \prod_{r_i \in \Phi}^{|r_i|<r} \exp \left( -2\mu_s \int_{\sqrt{r^2 - r_i^2}}^\infty \frac{sp_s (r_i^2 + u^2)^{-\frac{\beta}{2}}}{1 + sp_s (r_i^2 + u^2)^{-\frac{\beta}{2}}} du - 2\mu_r \int_{\sqrt{r^2 - r_i^2}}^\infty \frac{sp_r (r_i^2 + u^2)^{-\frac{\beta}{2}}}{1 + sp_r (r_i^2 + u^2)^{-\frac{\beta}{2}}} du \right) \\ & \quad \times \prod_{r_i \in \Phi}^{|r_i|>r} \exp \left( -2\mu_s \int_0^\infty \frac{sp_s (r_i^2 + u^2)^{-\frac{\beta}{2}}}{1 + sp_s (r_i^2 + u^2)^{-\frac{\beta}{2}}} du - 2\mu_r \int_0^\infty \frac{sp_r (r_i^2 + u^2)^{-\frac{\beta}{2}}}{1 + sp_r (r_i^2 + u^2)^{-\frac{\beta}{2}}} du \right). \quad (25) \end{aligned}$$

To get (a), we use the Laplace transform of the exponential random variable and the fact that conditionally on the line process and conditionally on the association distance  $r$ , all RSUs and relays are at distances greater than  $r$ . To obtain (b), we use the facts that RSU and relay point processes on different lines are conditionally independent and that the distances from the origin to any RSU points  $\{T_k\}_{k \in \mathbb{Z}} \in S_{r_i,\theta_i}$  are given by  $\{\sqrt{r_i^2 + G_k^2}\}_{k \in \mathbb{Z}}$ , where  $\{G_k\}_{k \in \mathbb{Z}}$  is the RSU Poisson point process on the real axis  $S_{0,0}$ .

On the other hand, the probability density function in Eq. (21) is given by

$$\begin{aligned}
\mathbf{P}(\|X_S^*\| \in [r, r + dr], E, A_s | \Phi) &= \frac{\partial(1 - \mathbf{P}(S_{0,\theta_0}(B_0(r)) = 0))}{\partial r} dr \\
&\quad \times \mathbf{P}(R_{0,\theta_0}(B(r)) = \emptyset) \prod_{r_i, \theta_i \in \Phi} \mathbf{P}(S_{r_i,\theta_i} + R_{r_i,\theta_i}(B(r)) = \emptyset) \\
&= 2\mu_s e^{-2r\mu_s} dr e^{-2r\mu_r} \prod_{r_i, \theta_i \in \Phi}^{r_i < r} e^{-2(\mu_s + \mu_r)\sqrt{r^2 - r_i^2}}, \tag{26}
\end{aligned}$$

where we use the facts that  $X_\star \in S_{0,\theta_0}$  and that there is no point of  $R_{0,\theta_0} + S_{r_i,\theta_i} + R_{r_i,\theta_i}$  within a disk of radius  $r$  centered at the origin. The probability density function in Eq. (22) is

$$\mathbf{P}(\|X_R^*\| \in (r, r + dr), E, A_r | \Phi) = 2\mu_r e^{-2r\mu_r} dr e^{-2r\mu_s} \prod_{r_i, \theta_i \in \Phi}^{r_i < r} e^{-2(\mu_s + \mu_r)\sqrt{r^2 - r_i^2}}. \tag{27}$$

To derive the first part of Eq. (19), we combine Eqs. (22)–(27) and obtain the product form based on the probability generating functional of the Poisson line process.

Let us now evaluate the second part of Eq. (19). By the law of total probability, we have

$$\mathbf{P}_U^0(\text{SIR} > \tau, E^c) = \mathbf{P}_U^0(\text{SIR} > \tau, E^c, A_s) + \mathbf{P}_U^0(\text{SIR} > \tau, E^c, A_r), \tag{28}$$

where  $A_s$  and  $A_r$  denote the events that the typical user is associated with the RSU or with the relay, respectively. Let  $l_\star$  denote the line of the association RSU transmitter. Then, by conditioning on  $\Phi$ , on  $l_\star$ , and then  $\|X_S^*\|$ , we can write the first part of Eq. (28) as follows:

$$\begin{aligned}
&\mathbf{P}_U^0(\text{SIR} > \tau, E^c, A_s) \\
&= \mathbf{P}_U^0(p_s H L(\|X^*\|) > \tau I, E^c, A_s) \\
&= \mathbf{P}_U^0(p_s H > \tau I \|X_\star\|^\beta, E^c, A_s) \\
&= \mathbf{E}_\Phi \left[ \mathbf{P}_U^0 \left( H > \frac{\tau I \|X_\star\|^\beta}{p_s}, E^c, A_s \middle| \Phi \right) \right] \\
&= \mathbf{E}_\Phi \left[ \mathbf{E}_{l_\star} \left[ \mathbf{P}_U^0 \left( H > \frac{\tau I \|X_S^*\|^\beta}{p_s}, E^c, A_s \middle| l_\star, \Phi \right) \right] \right] \\
&= \mathbf{E}_\Phi \left[ \mathbf{E}_{l_\star} \left[ \mathbf{E}_{\|X_S^*\|} \left[ \mathbf{P}_U^0 \left( H > \frac{\tau r^\beta I}{p_s} \middle| E^c, A_s, \|X_S^*\| = r, l_\star \Phi \right) \right] \right] \right]. \tag{29}
\end{aligned}$$

In a similar way, the second part of Eq. (28) can be written as follows:

$$\begin{aligned}
&\mathbf{P}_U^0(\text{SIR} > \tau, E^c, A_r) \\
&= \mathbf{E}_\Phi \left[ \mathbf{E}_{l_\star} \left[ \mathbf{E}_{\|X_S^*\|} \left[ \mathbf{P}_U^0 \left( H > \frac{\tau r^\beta I}{p_r} \middle| E^c, A_r, \|X_S^*\| = r, l_\star \Phi \right) \right] \right] \right]. \tag{30}
\end{aligned}$$

By using the fact that  $H$  is an exponential random variable, the conditional probability of Eq. (29) is given by

$$\begin{aligned}
\mathcal{L}_I(s) &= \mathbf{E}_I[e^{-s\bar{I}} | E^c, A_s, r, l_\star, \Phi] \\
&= \prod_{r_i, \theta_i}^{\Phi + \delta_{r_\star, \theta_\star} + \delta_{0, \theta_0}} \mathbf{E} \left[ \prod_{X_j \in R_{r_i, \theta_i} + S_{r_i, \theta_i}}^{\|X_j\| > r} \frac{1}{1 + p_{X_j} s L(\|X_j\|)} \right] \\
&= \prod_{r_i, \theta_i}^{\Phi + \delta_{r_\star, \theta_\star} + \delta_{0, \theta_0}} \left( \mathbf{E} \left[ \prod_{T_j \in S_{0,0}}^{|T_j| > \sqrt{r^2 - r_i^2}} \frac{1}{1 + p_s s L(\|r_i \vec{e}_{i,1} + T_j \vec{e}_{i,2}\|)} \right] \right. \\
&\quad \left. \mathbf{E} \left[ \prod_{T_j \in R_{0,0}}^{|T_j| > \sqrt{r^2 - r_i^2}} \frac{1}{1 + p_r s L(\|r_i \vec{e}_{i,1} + T_j \vec{e}_{i,2}\|)} \right] \right), \quad (31)
\end{aligned}$$

where the distances from the origin to the points of the Poisson point process on line  $l(r_i, \theta_i)$  are represented by  $\|r_i \vec{e}_1 + T_j \vec{e}_2\|$  where  $\vec{e}_{i,1}$  is an orthonormal vector from the origin to the line  $l(r_i, \theta_i)$  and  $\vec{e}_{i,2}$  is an unit vector orthogonal to the vector  $\vec{e}_{i,1}$ . Here,  $S_{0,0}$  is the RSU point process on the  $x$ -axis and  $R_{0,0}$  is the relay point process on the  $x$ -axis. By using the probability generating functional of the Poisson point process, we get

$$\begin{aligned}
\mathcal{L}_I(s) &= \exp \left( -2\mu_s \int_r^\infty \frac{p_s s v^{-\alpha}}{1 + p_s s v^{-\alpha}} dv - 2\mu_r \int_r^\infty \frac{p_r s v^{-\alpha}}{1 + p_r s v^{-\alpha}} dv \right) \\
&\times \prod_{r_i, \theta_i \in \Phi + \delta_{r_\star, \theta_\star}}^{|r_i| < r} \exp \left( -2\mu_s \int_{\sqrt{r^2 - r_i^2}}^\infty \frac{p_s s (r_i^2 + v^2)^{-\frac{\beta}{2}}}{1 + p_s s (r_i^2 + v^2)^{-\frac{\beta}{2}}} dv \right) \\
&\times \prod_{r_i, \theta_i \in \Phi + \delta_{r_\star, \theta_\star}}^{|r_i| < r} \exp \left( -2\mu_r \int_{\sqrt{r^2 - r_i^2}}^\infty \frac{p_r s (r_i^2 + v^2)^{-\frac{\beta}{2}}}{1 + p_r s (r_i^2 + v^2)^{-\frac{\beta}{2}}} dv \right) \\
&\times \prod_{r_i, \theta_i \in \Phi}^{|r_i| > r} \exp \left( -2\mu_s \int_0^\infty \frac{p_s s (r_i^2 + v^2)^{-\frac{\beta}{2}}}{1 + p_s s (r_i^2 + v^2)^{-\frac{\beta}{2}}} dv \right) \\
&\times \prod_{r_i, \theta_i \in \Phi}^{|r_i| > r} \exp \left( -2\mu_r \int_0^\infty \frac{p_r s (r_i^2 + v^2)^{-\frac{\beta}{2}}}{1 + p_r s (r_i^2 + v^2)^{-\frac{\beta}{2}}} dv \right), \quad (32)
\end{aligned}$$

where the above terms are the Laplace transforms of the RSU plus relay interference on the line  $l(0, \theta_0)$ , the RSU interference on the lines closer than  $r$ , the relay interference on the lines closer than  $r$ , the RSU interference on the lines further than  $r$ , and the relay interference on the lines further than  $r$ , respectively.

To obtain the conditional probability density function of the distance from the origin to its closest RSU in Eq. (29), we use the facts that (i)  $X_S^*$  is the closest to the origin, (ii)  $X_S^* \in S_{r_\star, \theta_\star}$ ,

and (iii) all the other RSU or relay point processes have no point in the disk of radius  $r$ . Therefore, using the void probability of the Poisson point process, the conditional probability density function of the distance from the origin to its closest RSU in Eq. (29) is

$$\begin{aligned} \mathbf{P}_U^0(\|X_S^*\| \in [r, r + dr], E^c, A_s | l^*, \Phi) &= \frac{d}{dr} (1 - \mathbf{P}(S_{r^*, \theta^*}(B(r)) = \emptyset)) dr \mathbf{P}(R_{r^*, \theta^*}(B(r)) = \emptyset) \\ &\quad \times \left( \prod_{r, \theta}^{\Phi+l_0} \mathbf{P}(R_{r, \theta} + S_{r, \theta}(B(r)) = \emptyset) \right) \\ &= \frac{2\mu_s r e^{-2(\mu_s + \mu_r) \sqrt{r^2 - r_*^2}}}{\sqrt{r^2 - r_*^2}} dr \prod_{r_i, \theta_i}^{\Phi+\delta_{0, \theta_0}} e^{-2(\mu_s + \mu_r) \sqrt{r^2 - r_i^2}}. \end{aligned} \quad (33)$$

In a similar way, the conditional probability density function of the distance from the origin to its closest vehicle relay in Eq. (30) is given by

$$\mathbf{P}_U^0(\|X_S^*\| \in [r, r + dr], E^c, A_r | l^*, \Phi) = \frac{2\mu_r r e^{-2(\mu_s + \mu_r) \sqrt{r^2 - r_*^2}}}{\sqrt{r^2 - r_*^2}} dr \prod_{r_i}^{\Phi+\delta_{0, \theta_0}} e^{-2(\mu_s + \mu_r) \sqrt{r^2 - r_i^2}}. \quad (34)$$

Finally, we combine Eqs. (32) and (33) then integrate the result w.r.t.  $l^*$  and then w.r.t.  $\Phi$ . First, to integrate w.r.t.  $l^*$ , we combine all the functions w.r.t.  $l^*$  to get the following expression:

$$\begin{aligned} \mathbf{E}_{l^*} &\left[ \frac{2\mu_s r e^{-2(\mu_s + \mu_r) \sqrt{r^2 - r_*^2}} e^{-2\mu_s \int_{\sqrt{r^2 - r_*^2}}^{\infty} \frac{p_{ss}(r_*^2 + v^2)^{-\frac{\beta}{2}}}{1 + p_{ss}(r_*^2 + v^2)^{-\frac{\beta}{2}}} dv} e^{-2\mu_r \int_{\sqrt{r^2 - r_*^2}}^{\infty} \frac{p_{rs}(r_*^2 + v^2)^{-\frac{\beta}{2}}}{1 + p_{rs}(r_*^2 + v^2)^{-\frac{\beta}{2}}} dv}}{\sqrt{r^2 - r_*^2}} \right] \\ &= 4\lambda_l \mu_s r \int_0^r \frac{e^{-2(\mu_s + \mu_r) \sqrt{r^2 - z^2}} e^{-2\mu_s \int_{\sqrt{r^2 - z^2}}^{\infty} \frac{p_{ss}(z^2 + v^2)^{-\frac{\beta}{2}}}{1 + p_{ss}(z^2 + v^2)^{-\frac{\beta}{2}}} dv} e^{-2\mu_r \int_{\sqrt{r^2 - z^2}}^{\infty} \frac{p_{rs}(z^2 + v^2)^{-\frac{\beta}{2}}}{1 + p_{rs}(z^2 + v^2)^{-\frac{\beta}{2}}} dv}}{\sqrt{r^2 - z^2}} dz \\ &= 4\lambda_l \mu_s r \int_0^{\pi/2} e^{-2r(\mu_s + \mu_r) \sin(\theta) - \int_{r \sin(\theta)}^{\infty} \frac{2\mu_s s p_s(r^2 \cos^2(\theta) + v^2)^{-\frac{\beta}{2}}}{1 + s p_s(r^2 \cos^2(\theta) + v^2)^{-\frac{\beta}{2}}} dv - \int_{r \sin(\theta)}^{\infty} \frac{2\mu_r s p_r(r^2 \cos^2(\theta) + v^2)^{-\frac{\beta}{2}}}{1 + s p_r(r^2 \cos^2(\theta) + v^2)^{-\frac{\beta}{2}}} dv} d\theta, \end{aligned} \quad (35)$$

where we use Campbell's average formula [34] and then replace the variable  $z$  with  $r \cos(\theta)$ . We combine Eqs. (32), (33), and (35) to obtain the first part of Eq. (28).

Similarly, to obtain the second part of Eq. (28), we combine Eq. (32) and (34) and evaluate the functions w.r.t.  $l^*$  to obtain the following expression:

$$4\lambda_l \mu_r r \int_0^{\pi/2} e^{-2r(\mu_s + \mu_r) \sin(\theta) - \int_{r \sin(\theta)}^{\infty} \frac{2\mu_s s p_s(r^2 \cos^2(\theta) + v^2)^{-\frac{\beta}{2}}}{1 + s p_s(r^2 \cos^2(\theta) + v^2)^{-\frac{\beta}{2}}} dv - \int_{r \sin(\theta)}^{\infty} \frac{2\mu_r s p_r(r^2 \cos^2(\theta) + v^2)^{-\frac{\beta}{2}}}{1 + s p_r(r^2 \cos^2(\theta) + v^2)^{-\frac{\beta}{2}}} dv} d\theta. \quad (36)$$

Then, we combine the rest of Eq. (32), (34) and (36) to obtain the second part of Eq. (28). ■

**Corollary 1.** When  $p_s = p_r$ , or  $\gamma = 1$ , the SIR distribution of the typical user is

$$\begin{aligned} & \int_0^\infty J_1(r) e^{-2\lambda_l \int_0^r 1 - J_2(r, v) dv} e^{-2\lambda_l \int_r^\infty 1 - J_3(r, v) dv} dr \\ & + \int_0^\infty K_1(r) e^{-2\lambda_l \int_0^r 1 - K_2(r, v) dv} e^{-2\lambda_l \int_r^\infty 1 - K_3(r, v) dv} K_4(r) dr, \end{aligned} \quad (37)$$

where

$$\begin{aligned} J_1(r) &= 2(\mu_s + \mu_r) e^{-2r(\mu_s + \mu_r) - 2(\mu_s + \mu_r) \int_r^\infty \frac{\tau r^\alpha u^{-\alpha}}{1 + \tau r^\alpha u^{-\alpha}} du}, \\ J_2(r, v) &= e^{-2(\mu_s + \mu_r) \sqrt{r^2 - v^2} - 2(\mu_s + \mu_r) \int_{\sqrt{r^2 - v^2}}^\infty \frac{\tau r^\alpha (v^2 + u^2)^{-\frac{\beta}{2}}}{1 + \tau r^\alpha (v^2 + u^2)^{-\frac{\beta}{2}}} du}, \\ J_3(r) &= e^{-2(\mu_s + \mu_r) \int_0^\infty \frac{\tau r^\alpha (v^2 + u^2)^{-\beta/2}}{1 + \tau r^\alpha (v^2 + u^2)^{-\beta/2}} du}, \end{aligned}$$

and

$$\begin{aligned} K_1(r) &= e^{-2(\mu_s + \mu_r)r - 2(\mu_s + \mu_r) \int_r^\infty \frac{\tau r^\beta u^{-\alpha}}{1 + \tau r^\beta u^{-\alpha}} du}, \\ K_2(r, v) &= e^{-2(\mu_s + \mu_r) \sqrt{r^2 - v^2} - 2(\mu_s + \mu_r) \int_{\sqrt{r^2 - v^2}}^\infty \frac{\tau r^\beta (v^2 + u^2)^{-\beta/2}}{1 + \tau r^\beta (v^2 + u^2)^{-\beta/2}} du}, \\ K_3(r) &= e^{-2(\mu_s + \mu_r) \int_0^\infty \frac{\tau r^\beta (v^2 + u^2)^{-\beta/2}}{1 + \tau r^\beta (v^2 + u^2)^{-\beta/2}} du}, \\ K_4(r) &= 4\lambda_l(\mu_s + \mu_r)r \int_0^{\pi/2} e^{-2(\mu_s + \mu_r)r \sin(\theta) - 2(\mu_s + \mu_r) \int_{r \sin(\theta)}^\infty \frac{\tau r^\beta (r^2 \cos^2(\theta) + v^2)^{-\beta/2}}{1 + \tau r^\beta (r^2 \cos^2(\theta) + v^2)^{-\beta/2}} dv} d\theta. \end{aligned}$$

*Proof:* The proof is immediate by taking  $\gamma = 1$  in Theorem 2. ■

Since we analyze the performance of the user located at the origin—leveraging the stationary user point process, the obtained formula also corresponds to the spatial average of SIRs of all users in a large ball of the proposed network [34], [43]. In addition, if we consider a simple dynamic where users are assumed to move at a constant speed along the lines that they are located on, the locations of users at any given time follow a Poisson point process on each line (displacement Theorem [34]). Therefore, the locations of all users in the network at any given time follow a Cox point process  $U$ . More precisely, the user point process is time-invariant. Therefore, the SIR distribution of the typical user also coincides with the SIR distribution of a specific user, averaged over a very long time [44].

Fig. 5 and 6 show that the derived formula matches the numerical results obtained by Monte Carlo simulations. To get the simulation results, we consider a disk of radius  $R = 5$  km and fix the SIR threshold  $\tau$ . Then, for each simulation sample  $k = 1, 2, \dots, N$ , randomly oriented Poisson( $2\lambda_l R$ ) lines are distributed on the disk and corresponding RSU and relays are distributed.

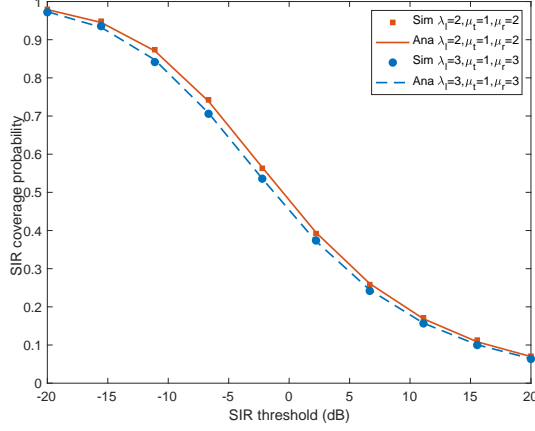


Fig. 5. SIR coverage probability, namely the probability that the typical user at the origin has a SIR greater than a given threshold. For various network parameters, we show that the derived formula matches the simulation results. Here, we use  $\gamma = 1$ ,  $\alpha = 2.5$  and  $\beta = 3.5$ . The units of parameters  $\lambda_l$ ,  $\mu_s$ , and  $\mu_r$  are per kilometer.

Since the network performance is investigated through the typical user at the origin, a randomly oriented line exists and this line contains the origin, RSUs, and relays. In each simulation sample  $k$ , Rayleigh fading, path losses for desired signal and interference, and penetration loss are considered to assess whether the SIR of the user at the origin exceeds the SIR threshold  $\tau$ . Then, the probability of the SIR being greater than  $\tau$  is obtained by counting the number of such instances divided by the total number  $N$ . We vary  $\tau$  to obtain the SIR curve. The accuracy of the Monte Carlo method increases as the total number of instances  $N$  increases, together with the complexity and computation cost. In this paper, we consider  $N = 10^5$  samples and  $R = 5$  km to obtain the Monte Carlo simulation results.

Figs. 7 – 10 show the SIR distribution, or the SIR coverage probability of the typical user. For clearer plots, only analytical results are illustrated. Fig. 7 shows the behavior of SIR as more relays are added when the road density is fixed. Since  $\mu_s = 1$ ,  $\mu_r$  denotes both the relative number of relays per a kilometer length of a road and the average relay per RSU. In this numerical experiment, different path loss exponents are assumed for intra-road links and inter-road links, i.e.,  $\alpha \neq \beta$ . Note that in Figs. 6 and 7 and the SIR hardly change as the density of the relays varies.

Figs. 8 and 9 show the typical SIR coverage probability for different road densities. In both figures,  $\lambda_l$  increases and this means the number of roads per unit area increases. Since RSUs

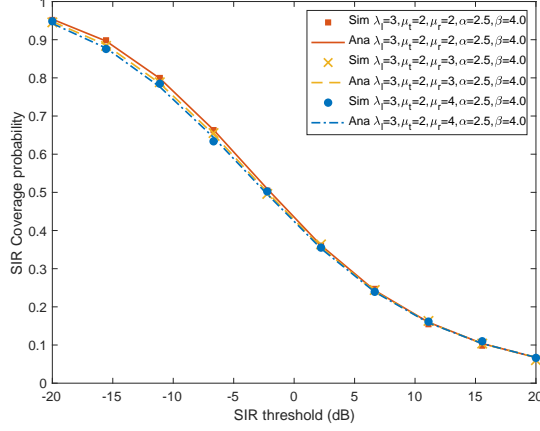


Fig. 6. SIR coverage probability of the typical user. We consider  $\gamma = 1$ ,  $\alpha = 2.5$  and  $\beta = 4$ .

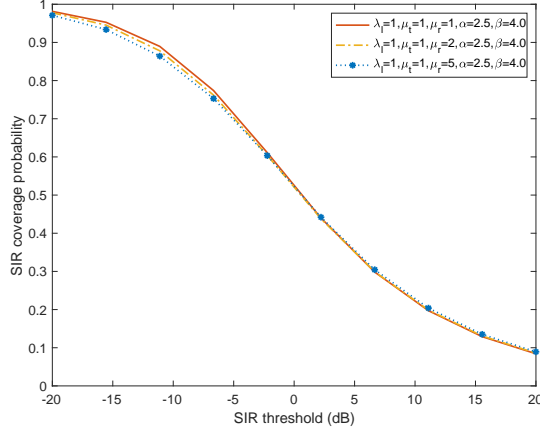


Fig. 7. SIR coverage probability of the typical user. We increase the density of relays in the proposed network to study the behavior of the SIR coverage probability. Only curves based on analytical formula are given.

and relays are distributed as Poisson point processes on each line, the total numbers of RSUs and relays per unit area increases. In both figures, an increment of the road density decreases the SIR coverage probability of the typical user. Fig. 9 analyzes the impact of deploying more relays when the density of roads is high. We compare the result with Fig. 7 and see that as the density of roads increases, the interference increases and the SIR coverage probability of the typical user decreases.

Fig. 10 uses the same path loss exponents for all links, namely  $\alpha = \beta$ . By comparing Figs. 9 and 10, we see that, as the density of roads increases, the SIRs decrease less for  $\alpha = \beta$  than for

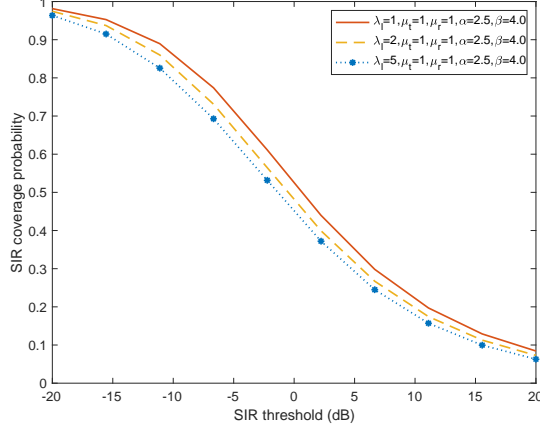


Fig. 8. SIR coverage probability of the typical user. We increase the density of roads in the proposed network.  $\gamma = 1$ .

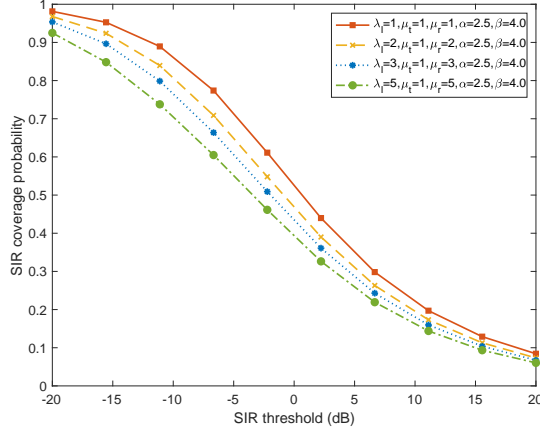


Fig. 9. SIR coverage probability of the typical user. We increase the density of roads in the proposed network.  $\gamma = 1$ .

$\alpha \neq \beta$ . This occurs because as the density of roads increases, users are likely to be associated with RSUs or relays on different roads. As a result, when  $\beta = \alpha = 2.5$ , the association transmitter on a different line offers a stronger received signal power than when  $\beta = 4$  and  $\alpha = 2.5$ .

**Remark 1.** *From Theorem 2, all communications in the proposed heterogeneous vehicular*

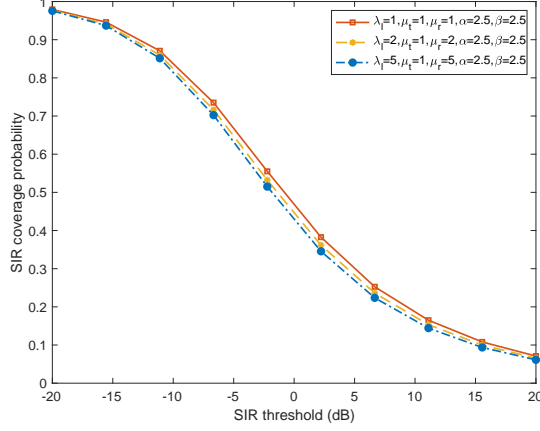


Fig. 10. SIR coverage probability of the typical user. We use  $\gamma = 1$ .

network can be divided into the following four types:

$\mathbf{P}(\text{SIR} > \tau | A_s, E)$  : SIR dist. of the typical user associated with an RSU on the same line

$\mathbf{P}(\text{SIR} > \tau | A_r, E)$  : SIR dist. of the typical user associated with a relay on the same line

$\mathbf{P}(\text{SIR} > \tau | A_s, E^c)$  : SIR dist. of the typical user associated with an RSU on a different line

$\mathbf{P}(\text{SIR} > \tau | A_r, E^c)$  : SIR dist. of the typical user associated with a relay on a different line,

The formulas for these four different types can be simply obtained from the expressions in Theorem 2. Note that these four types cover all the links based on their type or geometry. For instance,  $\mathbf{P}(\text{SIR} > \tau | A_s, E^c)$  gives the reliability of cross-road RSU-to-user performance and  $\mathbf{P}(\text{SIR} > \tau | A_r, E)$  gives the reliability of same road relay-to-user performance. As a function of various large-scale parameters such as densities, path loss exponents, and transmit powers, this geometry-based analysis for each type will shed light on the type-specific reliability, on tradeoff relationship between link types, and on a asymptotic behavior of users.

### C. SIR Distribution of the Typical Relay

In practice, relays can only communicate with users on the downlink, once the relevant data are communicated through RSU-to-relay links. To evaluate the user performance accounting for RSU-to-relay links, this section now analyzes the SIR distribution of RSU-to-relay links, namely the SIR distribution of the typical relay at the origin.

**Theorem 3.** *The SIR distribution of the typical relay is given by*

$$\begin{aligned} & \int_0^\infty \bar{J}_1(r) e^{-2\lambda_l \int_0^r 1 - \bar{J}_2(r, v) dv} e^{-2\lambda_l \int_r^\infty 1 - \bar{J}_3(r, v) dv} dr \\ & + \int_0^\infty \bar{K}_1(r) e^{-2\lambda_l \int_0^r 1 - \bar{K}_2(r, v) dv} e^{-2\lambda_l \int_r^\infty 1 - \bar{K}_3(r, v) dv} \bar{K}_4(r) dr, \end{aligned} \quad (38)$$

where

$$\begin{aligned} \bar{J}_1(r) &= 2\mu_s e^{-2r\mu_s - 2\mu_s \int_r^\infty \frac{\tau r^{\alpha} u^{-\alpha}}{1+\tau r^{\alpha} u^{-\alpha}} du}, \\ \bar{J}_2(r, v) &= e^{-2\mu_s \sqrt{r^2 - v^2} - 2\mu_s \int_{\sqrt{r^2 - v^2}}^\infty \frac{\tau r^{\alpha} (v^2 + u^2)^{-\frac{\beta}{2}}}{1+\tau r^{\alpha} (v^2 + u^2)^{-\frac{\beta}{2}}} du}, \\ \bar{J}_3(r) &= e^{-2\mu_s \int_0^\infty \frac{\tau r^{\alpha} (v^2 + u^2)^{-\beta/2}}{1+\tau r^{\alpha} (v^2 + u^2)^{-\beta/2}} du}, \end{aligned}$$

and

$$\begin{aligned} \bar{K}_1 &= e^{-2r\mu_s - 2\mu_s \int_r^\infty \frac{\tau r^{\beta} u^{-\alpha}}{1+\tau r^{\beta} u^{-\alpha}} du}, \\ \bar{K}_2(r, v) &= e^{-2\mu_s \sqrt{r^2 - v^2} - 2\mu_s \int_{\sqrt{r^2 - v^2}}^\infty \frac{\tau r^{\beta} (v^2 + u^2)^{-\beta/2}}{1+\tau r^{\beta} (v^2 + u^2)^{-\beta/2}} du}, \\ \bar{K}_3(r) &= e^{-2\mu_s \int_0^\infty \frac{\tau r^{\beta} (v^2 + u^2)^{-\beta/2}}{1+\tau r^{\beta} (v^2 + u^2)^{-\beta/2}} du}, \\ \bar{K}_4(r) &= 4\lambda_l \mu_s r \int_0^{\pi/2} e^{-2\mu_s r \sin(\theta) - 2\mu_s \int_{r \sin(\theta)}^\infty \frac{\tau r^{\beta} (r^2 \cos^2(\theta) + v^2)^{-\beta/2}}{1+\tau r^{\beta} (r^2 \cos^2(\theta) + v^2)^{-\beta/2}} dv} d\theta. \end{aligned}$$

*Proof:* Here, the SIR distribution of the typical relay can be derived by employing the same techniques as in the proof of Theorem 2. ■

#### D. Average Effective User Rates

In the network, users are divided into those associated with RSUs and those associated with relays. First, the average effective rate of RSU-associated users is defined by the mean achievable rate of the typical RSU associated users divided by the mean number of users per RSU. The average effective rate of the RSU-associated user is given by

$$\mathcal{T}_s = \frac{W_1 \mathbf{E}[\log_2(1 + \text{SIR}_{s \rightarrow u})]}{\mathbf{E}[\# \text{ users per RSU}]} \quad (39)$$

Note the effective user rate metric is in a sense heuristic because it is given by the ratio of the mean Shannon rate to the mean number of associated users, not the exact number of associated users. However, the exact distribution of the Voronoi cell of Cox-Voronoi tessellation is unknown; and thus dividing the sum of Shannon rates by the exact number of associated users is currently

infeasible. Based on the mass transport, we obtained the mean number of users in the typical cell (Proposition 1) and we now use it for computing the average effective rate.

The average effective rate of relay-associated users is determined by both the RSU-to-relay and relay-to-user links. Using the average effective rates of the both links, the mean effective rate of the relay-associated user is defined by

$$\mathcal{T}_r = \min \left\{ \frac{W_2 \mathbf{E}[\log_2(1 + \text{SIR}_{s \rightarrow r})]}{\mathbf{E}[\# \text{ relay per RSU}] \mathbf{E}[\# \text{ user per relay}]}, \frac{W_1 \mathbf{E}[\log_2(1 + \text{SIR}_{r \rightarrow u})]}{\mathbf{E}[\# \text{ user per relay}]} \right\}, \quad (40)$$

where  $W_2$  is the bandwidth for the RSU-to-relay communications and  $W_1$  is the bandwidth for RSU-to-user and relay-to-user communications.

We combine Eqs. (39) and (40) to derive the average effective rate of the typical user:

$$\mathcal{T} = \mathbf{P}_U^0(A_s) \mathcal{T}_s + \mathbf{P}_U^0(A_r) \mathcal{T}_r. \quad (41)$$

Here,  $\mathbf{P}(A_s)$  is the probability that the typical user is associated with an RSU, provided in Theorem 1.

**Theorem 4.** *The average effective rate of the typical user is*

$$\begin{aligned} \mathcal{T} = & \mathbf{P}_U^0(A_s) W_1 \int_0^\infty \frac{\mathbf{P}_U^0(\text{SIR}_{s \rightarrow u} > 2^\xi - 1)}{\bar{u}_s} d\xi \\ & + \mathbf{P}_U^0(A_r) \min \left\{ \int_0^\infty \frac{W_2 \mathbf{P}_U^0(\text{SIR}_{s \rightarrow r} > 2^\xi - 1)}{\bar{r}_s \bar{u}_r} d\xi, \int_0^\infty \frac{W_1 \mathbf{P}_U^0(\text{SIR}_{r \rightarrow u} > 2^\xi - 1)}{\bar{u}_r} d\xi \right\}, \end{aligned} \quad (42)$$

where  $\mathbf{P}_U^0(A_s)$  and  $\mathbf{P}_U^0(\text{SIR}_{s \rightarrow r} > 2^\xi - 1)$  are given by Theorems 1 and 3, respectively. Using the functions in Theorem 2, the SIR distribution of the RSU-associated typical user is given by

$$\begin{aligned} & \mathbf{P}_U^0(\text{SIR}_{s \rightarrow u} > \tau) \\ &= \frac{1}{\mathbf{P}_U^0(\mathcal{A}_s)} \int_0^\infty G_1(r, a, b) e^{-2\lambda_l \int_0^r 1 - G_2(r, v, a, b) dv - 2\lambda_l \int_r^\infty 1 - G_3(r, v, a, b) dv} dr \Big|_{a=1, b=\frac{1}{\gamma}} \\ &+ \frac{1}{\mathbf{P}_U^0(\mathcal{A}_s)} \int_0^\infty H_1(r, a, b) e^{-2\lambda_l \int_0^r 1 - H_2(r, v, a, b) dv - 2\lambda_l \int_r^\infty 1 - H_3(r, v, a, b) dv} H_4(r, a, b) dr \Big|_{a=1, b=\frac{1}{\gamma}, c=\mu_s}. \end{aligned}$$

Similarly, the SIR distribution of the relay-associated typical user is given by

$$\begin{aligned} & \mathbf{P}_U^0(\text{SIR}_{r \rightarrow u} > \tau) \\ &= \frac{1}{\mathbf{P}_U^0(\mathcal{A}_r)} \int_0^\infty G_1(r, a, b) e^{-2\lambda_l \int_0^r 1 - G_2(r, v, a, b) dv - 2\lambda_l \int_r^\infty 1 - G_3(r, v, a, b) dv} dr \Big|_{a=\gamma, b=1} \\ &+ \frac{1}{\mathbf{P}_U^0(\mathcal{A}_r)} \int_0^\infty H_1(r, a, b) e^{-2\lambda_l \int_0^r 1 - H_2(r, v, a, b) dv - 2\lambda_l \int_r^\infty 1 - H_3(r, v, a, b) dv} \bar{H}_4(r, a, b) dr \Big|_{a=\gamma, b=1, c=\mu_r}. \end{aligned}$$

We have  $\bar{u}_s = \frac{\mu_u}{\mu_s} \mathbf{P}_U^0(A_s)$ ,  $\bar{u}_r = \frac{\mu_u}{\mu_r} \mathbf{P}_U^0(A_r)$ , and  $\bar{r}_s = \frac{\mu_r}{\mu_s}$  from Proposition 1.

*Proof:* The coverage probabilities of the typical RSU-to-user link and of the typical relay-to-user link are obtained by leveraging Theorem 2, respectively. We have

$$\mathbf{P}_U^0(\text{SIR}_{s \rightarrow u} > \tau) := \mathbf{P}_U^0(\text{SIR} > \tau | A_s) = \frac{\mathbf{P}_U^0(\text{SIR} > \tau, A_s, E) + \mathbf{P}_U^0(\text{SIR} > \tau, A_s, E^c)}{\mathbf{P}_U^0(A_s)},$$

$$\mathbf{P}_U^0(\text{SIR}_{r \rightarrow u} > \tau) := \mathbf{P}_U^0(\text{SIR} > \tau | A_r) = \frac{\mathbf{P}_U^0(\text{SIR} > \tau, A_r, E) + \mathbf{P}_U^0(\text{SIR} > \tau, A_r, E^c)}{\mathbf{P}_U^0(A_r)}.$$

To obtain  $\bar{u}_s, \bar{u}_r$ , and  $\bar{r}_s$ , we use Proposition 1. This completes the proof.  $\blacksquare$

**Example 1.** Suppose  $\gamma = 1$  and  $W_2$  is sufficiently. Then, the average effective rate is

$$\mathcal{T} = W_1 \int_0^\infty \frac{\mu_s \mathbf{P}_U^0(\text{SIR}_{S \rightarrow U} > 2^\xi - 1)}{\mu_u} d\xi + W_1 \int_0^\infty \frac{\mu_r \mathbf{P}_U^0(\text{SIR}_{R \rightarrow U} > 2^\xi - 1)}{\mu_u} d\xi. \quad (43)$$

On the other hand, without any relay in the network, the average effective user rate is

$$\left( \frac{\mu_s}{\mu_u} \right) W_1 \int_0^\infty \mathbf{P}_U^0(\text{SIR} > 2^\xi - 1) d\xi. \quad (44)$$

As a result, the proposed network with relays gives a multiplicative gain of

$$\Gamma = \frac{\int_0^\infty \mathbf{P}_U^0(\text{SIR}_{S \rightarrow U} > 2^\xi - 1) d\xi}{\int_0^\infty \mathbf{P}_U^0(\text{SIR} > 2^\xi - 1) d\xi} + \left( \frac{\mu_r}{\mu_s} \right) \frac{\int_0^\infty \mathbf{P}_U^0(\text{SIR}_{R \rightarrow U} > 2^\xi - 1) d\xi}{\int_0^\infty \mathbf{P}_U^0(\text{SIR} > 2^\xi - 1) d\xi} \quad (45)$$

Fig. 11 illustrates the gain of the average effective user rate as the density of relays increases. It shows how the gain behaves as the density of relays increases.

**Remark 2.** Theorem 4 represents the mean effective rate as a function of  $W_1, W_2$ , and the distributions of  $\text{SIR}_{S \rightarrow U}$ ,  $\text{SIR}_{R \rightarrow U}$ , and  $\text{SIR}_{S \rightarrow R}$ . Then, when  $W_2$  is large, the representation shows that deploying relays will substantially increase the average effective rate of users. In practice,  $W_1$  and  $W_2$  are finite and the derived mean effective rate formula is useful to address various design problems present in heterogeneous vehicular networks. For instance, to maximize the mean effective user rate, one can find the optimal density of relays for a given  $W_2$ . Similarly, when the density of relays is given, one can use the effective rate formula to study the impact of  $W_2$ .

#### IV. CONCLUSION

Using stochastic geometry, this paper proposes and analyzes a novel 2-tier heterogeneous vehicular network architecture where RSUs and vehicle relays serve vehicle users. By modeling

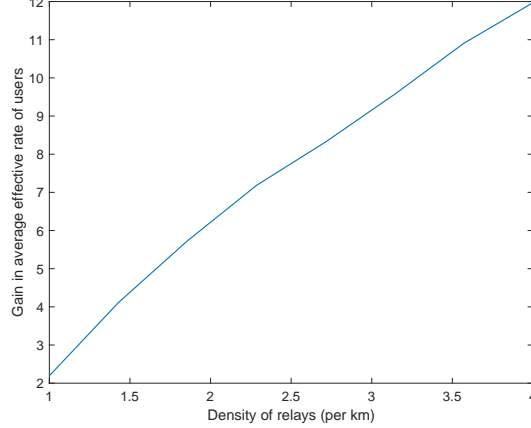


Fig. 11. Gains in the average effective user rate when  $W_2$  is very large. The gain is presented for  $\lambda_l = \mu_s = 1/\text{km}$ ,  $\mu_u = 10/\text{km}$ , and  $\alpha = \beta = 3$ . The analytic curve is based on Eq. (45).

the proposed network as the Cox point processes and by assuming the nearest association principle with a two-slopes attenuation model, we derive the probability that the typical user is associated with either an RSU or a relay. Then, we derive the SIR distribution of the typical user as an integral formula. We check that the derived analytic formulas match the simulation results obtained by the Monte-Carlo experiments. In addition, using the association probability and SIR distribution, we characterize the SIR distributions of all typical types of communications that exist in the network. Finally, based on the SIR distributions of all typical links and their corresponding bandwidths, we derive the average effective user rate. Finally, we characterize the gain in the effective user rate provided by the proposed network.

## REFERENCES

- [1] J. B. Kenney, “Dedicated short-range communications (DSRC) standards in the United States,” *Proceedings of the IEEE*, vol. 99, no. 7, pp. 1162–1182, July 2011.
- [2] J. Jin, J. Gubbi, S. Marusic, and M. Palaniswami, “An information framework for creating a smart city through Internet of Things,” *IEEE Internet Things J.*, vol. 1, no. 2, pp. 112–121, 2014.
- [3] N. Lu, N. Cheng, N. Zhang, X. Shen, and J. W. Mark, “Connected vehicles: Solutions and challenges,” *IEEE Internet Things J.*, vol. 1, no. 4, pp. 289–299, 2014.
- [4] D. Caveney, “Cooperative vehicular safety applications,” *IEEE Cont. Syst. Mag.*, vol. 30, no. 4, pp. 38–53, 2010.
- [5] S. Sivaraman and M. M. Trivedi, “Looking at vehicles on the road: A survey of vision-based vehicle detection, tracking, and behavior analysis,” *IEEE Trans. Intell. Transp. Syst.*, vol. 14, no. 4, pp. 1773–1795, 2013.

- [6] A. Tahmasbi-Sarvestani, H. Nourkhiz Mahjoub, Y. P. Fallah, E. Moradi-Pari, and O. Abuchaar, "Implementation and evaluation of a cooperative vehicle-to-pedestrian safety application," *IEEE Intell. Transp. Syst. Mag.*, vol. 9, no. 4, pp. 62–75, 2017.
- [7] 3GPP TR 36.885, "Study on LTE-based V2X services," *3GPP TR 36.885*.
- [8] S. Chen, J. Hu, Y. Shi, Y. Peng, J. Fang, R. Zhao, and L. Zhao, "Vehicle-to-everything (V2X) services supported by LTE-based systems and 5G," *IEEE Commun. Standards Mag.*, vol. 1, no. 2, pp. 70–76, 2017.
- [9] D. Garcia-Roger, E. E. González, D. Martín-Sacristán, and J. F. Monserrat, "V2X support in 3GPP specifications: From 4G to 5G and beyond," *IEEE Access*, vol. 8, pp. 190 946–190 963, 2020.
- [10] 3GPP TS 22.816, "Service requirements for enhanced V2X scenarios," *3GPP TS 22.816*.
- [11] S.-Y. Lien, D.-J. Deng, C.-C. Lin, H.-L. Tsai, T. Chen, C. Guo, and S.-M. Cheng, "3GPP NR sidelink transmissions toward 5G V2X," *IEEE Access*, vol. 8, pp. 35 368–35 382, 2020.
- [12] K. Ganeshan, J. Lohr, P. B. Mallick, A. Kunz, and R. Kuchibhotla, "NR sidelink design overview for advanced V2X service," *IEEE Internet Things Mag.*, vol. 3, no. 1, pp. 26–30, 2020.
- [13] 3GPP TR 38.836, "Study on NR sidelink relay," *3GPP TR 38.836*.
- [14] 3GPP TR 38.874, "NR; study on integrated access and backhaul," *3GPP TR 38.874*.
- [15] M. H. C. Garcia, A. Molina-Galan, M. Boban, J. Gozalvez, B. Coll-Perales, T. Şahin, and A. Kousaridas, "A tutorial on 5G NR V2X communications," *arXiv preprint arXiv:2102.04538*, 2021.
- [16] I. Shayea, M. Ergen, M. Hadri Azmi, S. Aldirmaz Çolak, R. Nordin, and Y. I. Daradkeh, "Key challenges, drivers and solutions for mobility management in 5G networks: A survey," *IEEE Access*, vol. 8, pp. 172 534–172 552, 2020.
- [17] S. C. Ng, W. Zhang, Y. Zhang, Y. Yang, and G. Mao, "Analysis of access and connectivity probabilities in vehicular relay networks," *IEEE J. Sel. Areas Commun.*, vol. 29, no. 1, pp. 140–150, 2011.
- [18] Q. L. Gall, B. Błaszczyzyn, E. Cali, and T. En-Najjary, "Relay-assisted device-to-device networks: Connectivity and urbanization opportunities," in *2020 IEEE Wireless Communications and Networking Conference (WCNC)*, 2020, pp. 1–7.
- [19] C. Tunc and S. S. Panwar, "Mitigating the impact of blockages in millimeter-wave vehicular networks through vehicular relays," *IEEE Open J. Intelligent Transportation Systems*, vol. 2, pp. 225–239, 2021.
- [20] I. Ullah, M. Z. Asghar, L. Bariah, S. Muhaidat, and J. Hämäläinen, "Performance evaluation of relaying with different relay selection schemes in 5G NR V2X communications," in *Proc. IEEE CommNet*, 2021, pp. 1–7.
- [21] F. Baccelli and S. Zuyev, "Stochastic geometry models of mobile communication networks," *Frontiers in queueing*, pp. 227–243, 1997.
- [22] F. Morlot, "A population model based on a Poisson line tessellation," in *Proc. IEEE WiOpt*, 2012, pp. 337–342.
- [23] F. Baccelli, B. Blaszczyzyn, and P. Muhlethaler, "An Aloha protocol for multihop mobile wireless networks," *IEEE Trans. Inf. Theory*, vol. 52, no. 2, pp. 421–436, Feb 2006.
- [24] 3GPP TR 38.901, "Study on evaluation methodology of new vehicle-to-everything (V2X) use cases for LTE and NR," *3GPP TR 37885*.
- [25] C.-S. Choi and F. Baccelli, "Poisson Cox point processes for vehicular networks," *IEEE Trans. Veh. Technol.*, vol. 67, no. 10, pp. 10 160–10 165, Oct 2018.
- [26] ———, "An analytical framework for coverage in cellular networks leveraging vehicles," *IEEE Trans. Commun.*, vol. 66, no. 10, pp. 4950–4964, Oct 2018.
- [27] V. V. Chetlur and H. S. Dhillon, "Coverage analysis of a vehicular network modeled as Cox process driven by Poisson line process," *IEEE Trans. Wireless Commun.*, vol. 17, no. 7, pp. 4401–4416, July 2018.
- [28] C.-S. Choi and F. Baccelli, "Spatial and temporal analysis of direct communications from static devices to mobile vehicles," *IEEE Trans. Wireless Commun.*, vol. 18, no. 11, pp. 5128–5140, 2019.

- [29] C.-S. Choi, F. Baccelli, and G. de Veciana, “Densification leveraging mobility: An IoT architecture based on mesh networking and vehicles,” in *Proc. IEEE/ACM MobiHoc*, 2018, p. 71–80.
- [30] J. P. Jeyaraj and M. Haenggi, “Cox models for vehicular networks: SIR performance and equivalence,” *IEEE Trans. Wireless Commun.*, vol. 20, no. 1, pp. 171–185, 2021.
- [31] C.-S. Choi and F. Baccelli, “Modeling and analysis of vehicle safety message broadcast in cellular networks,” *IEEE Trans. Wireless Commun.*, vol. 20, no. 7, pp. 4087–4099, 2021.
- [32] H. S. Dhillon, R. K. Ganti, F. Baccelli, and J. G. Andrews, “Modeling and analysis of K-tier downlink heterogeneous cellular networks,” *IEEE J. Sel. Areas Commun.*, vol. 30, no. 3, pp. 550–560, 2012.
- [33] S. N. Chiu, D. Stoyan, W. S. Kendall, and J. Mecke, *Stochastic geometry and its applications*. John Wiley & Sons, 2013.
- [34] F. Baccelli and B. Błaszczyzyn, “Stochastic geometry and wireless networks: volume I theory,” *Foundations and Trends in Networking*, vol. 3, no. 3–4, pp. 249–449, 2010.
- [35] A. Goldsmith, *Wireless communications*. Cambridge University Press, 2005.
- [36] 3GPP TR 38.211, “NR; physical channels and modulation,” *3GPP TR 38211*.
- [37] 3GPP TR 38.901, “NR; study on channel model for frequencies from 0.5 to 100 GHz,” *3GPP TR 38901*.
- [38] I. Sen and D. W. Matolak, “Vehicle–vehicle channel models for the 5-GHz band,” *IEEE Trans. Intelli. Transp. Syst.*, vol. 9, no. 2, pp. 235–245, 2008.
- [39] M. Boban, X. Gong, and W. Xu, “Modeling the evolution of line-of-sight blockage for V2V channels,” in *Proc. IEEE VTC*, 2016, pp. 1–7.
- [40] J. Moller, *Lectures on random Voronoi tessellations*. Springer & Verlag, 2012, vol. 87.
- [41] 3GPP TR 22.839, “Study on vehicle-mounted relays; stage 1,” *3GPP TR 22.839*.
- [42] D. J. Daley and D. Vere-Jones, *An introduction to the theory of point processes: volume II: general theory and structure*. Springer Science & Business Media, New York, 2007.
- [43] F. Baccelli and B. Błaszczyzyn, “Stochastic geometry and wireless networks: Volume II applications,” *Foundations and Trends in Networking*, vol. 4, no. 1–2, pp. 1–312, 2010.
- [44] F. Baccelli and P. Brémaud, *Elements of queueing theory: Palm Martingale calculus and stochastic recurrences*. Springer & Verlag, 2013, vol. 26.